The heat capacity of a natural monticellite and phase equilibria in the system CaO-MgO-SiO₂-CO₂*

Z. D. Sharp,[1] E. J. Essene,[1] L. M. Anovitz,[1] G. W. Metz,[1] E. F. Westrum, Jr.,[2]
B. S. Hemingway[3] and J. W. Valley[4]

[1] Department of Geological Sciences, University of Michigan, Ann Arbor, MI 48109, U.S.A.
[2] Department of Chemistry, University of Michigan, Ann Arbor, MI 48109, U.S.A.
[3] United States Geological Survey, 959 National Center, Reston, VA 22092, U.S.A.
[4] Department of Geology and Geophysics, University of Wisconsin, Madison, WI 53706, U.S.A.

Abstract—The heat capacity of a natural monticellite ($Ca_{1.00}Mg_{.91}Fe_{.09}Mn_{.01}Si_{0.99}O_{3.99}$) measured between 9.6 and 343 K using intermittent-heating, adiabatic calorimetry yields $C_p^0(298)$ and S_{298}^0 of 123.64 ± 0.18 and 109.44 ± 0.16 J·mol⁻¹ K⁻¹ respectively. Extrapolation of this entropy value to end-member monticellite results in an S_{298}^0 = 108.1 ± 0.2 J·mol⁻¹ K⁻¹. High-temperature heat-capacity data were measured between 340–1000 K with a differential scanning calorimeter. The high-temperature data were combined with the 290–350 K adiabatic values, extrapolated to 1700 K, and integrated to yield the following entropy equation for end-member monticellite (298–1700 K):
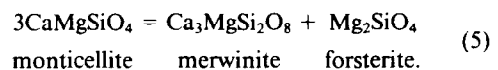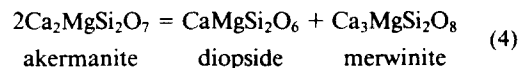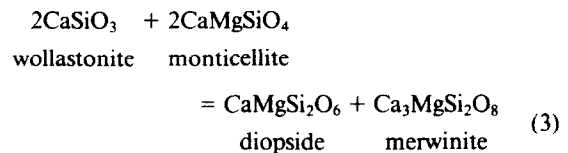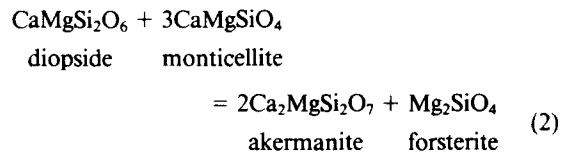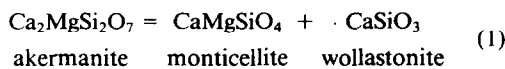
$$S_T^0 \,(\mathrm{J \cdot mol^{-1} \, K^{-1}}) = S_{298}^0 + 164.79 \ln T + 15.337 \cdot 10^{-3} \, T + 22.791 \cdot 10^5 \, T^{-2} - 968.94.$$

Phase equilibria in the CaO-MgO-SiO₂ system were calculated from 973 to 1673 K and 0 to 12 kbar with these new data combined with existing data for akermanite (*Ak*), diopside (*Di*), forsterite (*Fo*), merwinite (*Me*) and wollastonite (*Wo*). The location of the calculated reactions involving the phases *Mo* and *Fo* is affected by their mutual solid solution. A best fit of the thermodynamically generated curves to all experiments is made when the S_{298}^0 of *Me* is 250.2 J·mol⁻¹ K⁻¹, less than the measured value of 253.2 J·mol⁻¹ K⁻¹.

A best fit to the reversals for the solid-solid and decarbonation reactions in the CaO-MgO-SiO₂-CO₂ system was obtained with the ΔG_{298}^0 (kJ·mole⁻¹) for the phases *Ak* (−3667), *Di* (−3025), *Fo* (−2051), *Me* (−4317) and *Mo* (−2133). The two invariant points −*Wo* and −*Fo* for the solid-solid reactions are located at 1008 ± 5 K and 6.3 ± 0.1 kbar, and 1361 ± 10 K and 10.2 ± 0.2 kbar respectively. The location of the thermodynamically generated curves is in excellent agreement with most experimental data on decarbonation equilibria involving these phases.

INTRODUCTION

Bowen (1940) proposed ten decarbonation reactions in the system CaO-MgO-SiO₂-CO₂-H₂O characteristic of progressive metamorphism, which give rise to a petrogenetic grid in pressure-temperature space. Phase relations in the system CaO-MgO-SiO₂-*X*(CO₂) have since been carefully determined by experimental reversals at moderate pressures and temperatures. Unfortunately, efforts to match thermodynamically generated curves for the solid-solid reactions to the experimental reversals have not been entirely successful (Helgeson *et al.*, 1978; Valley and Essene, 1980), and thermodynamic arguments suggest that the experimental reversals for the decarbonation reactions must be in error (Turner, 1968). Valley and Essene (1980) fit thermodynamically derived curves to the experimental reversals for the following reactions:

$$\underset{\text{akermanite}}{Ca_2MgSi_2O_7} = \underset{\text{monticellite}}{CaMgSiO_4} + \underset{\text{wollastonite}}{CaSiO_3} \quad (1)$$

$$\underset{\text{diopside}}{CaMgSi_2O_6} + \underset{\text{monticellite}}{3CaMgSiO_4}$$
$$= \underset{\text{akermanite}}{2Ca_2MgSi_2O_7} + \underset{\text{forsterite}}{Mg_2SiO_4} \quad (2)$$

$$\underset{\text{wollastonite}}{2CaSiO_3} + \underset{\text{monticellite}}{2CaMgSiO_4}$$
$$= \underset{\text{diopside}}{CaMgSi_2O_6} + \underset{\text{merwinite}}{Ca_3MgSi_2O_8} \quad (3)$$

$$\underset{\text{akermanite}}{2Ca_2MgSi_2O_7} = \underset{\text{diopside}}{CaMgSi_2O_6} + \underset{\text{merwinite}}{Ca_3MgSi_2O_8} \quad (4)$$

$$\underset{\text{monticellite}}{3CaMgSiO_4} = \underset{\text{merwinite}}{Ca_3MgSi_2O_8} + \underset{\text{forsterite}}{Mg_2SiO_4}. \quad (5)$$

Experiments on reactions (2) and (4) could not be fit with available thermodynamic data for the end-member phases. Valley and Essene (1980) and Brousse *et al.* (1984) concluded that there must be errors in the entropies of monticellite and either merwinite or akermanite, assuming the reversed experiments are valid. At the time of these studies, the heat capacities of merwinite and akermanite had only been measured down to 50 K (Weller and Kelley, 1963), whereas the

heat capacity of monticellite was unmeasured. VALLEY and ESSENE (1980) used the value ½ S(forsterite) + ½ S(calcium-olivine) as their entropy estimate for monticellite. More recently, the heat capacity of akermanite has been measured between 9 and 1000 K (HEMINGWAY *et al.*, 1986) yielding an entropy 3.4 J · mol⁻¹ K⁻¹ higher than WELLER and KELLEY's (1963) estimate at 298°K.

VALLEY and ESSENE analyzed YODER's (1968) run products for reaction (4) in order to evaluate the degree of solid solution and found all phases to be stoichiometric within analytical error. The experiments of SCHAIRER *et al.* (1967) on the binary joins between akermanite and monticellite, forsterite, wollastonite, merwinite and diopside indicate that none of these phases has more than 1% solubility in akermanite. On the other hand, monticellite and forsterite exhibit significant mutual solid solution at high temperatures (BIGGAR and O'HARA, 1969; YANG, 1973; WARNER and LUTH, 1973; ADAMS and BISHOP, 1985), which potentially affects equilibrium reversals involving these phases. In order to refine phase relationships in the system CaO-MgO-SiO₂-CO₂, the volume and heat capacity of a natural monticellite were measured, and corrected for minor element substitution. The run products of YODER (1968) were analyzed to determine the degree of solid solution in akermanite, diopside, forsterite, merwinite and monticellite. With a measured entropy for monticellite, possible errors in the entropy of merwinite can be evaluated by fitting the thermodynamically generated curves to the experiments corrected for solid solutions.

MATERIALS

Ten grams of clear, glassy monticellite from Cascade Slide, NY (VALLEY and ESSENE, 1980) were separated for analysis. Chemical composition was determined with a fully automated CAMECA CAMEBAX microprobe at The University of Michigan (Table 1). The unit-cell volume of the natural material was determined by powder X-ray diffraction at ½°2θ/min. with quartz as an internal standard. A least-squares fit of the observed d values of unambiguously indexed peaks (Table 2) yielded the lattice parameters given in Table 3. The molar volume of end-member monticellite was calculated assuming a linear variation between the composition and molar volumes for the phases kirschsteinite, calcium olivine and tephroite (Table 4). The monticellite sample was presumed to be free of vacancies (*cf.* BROWN, 1982) and the analysis was

Table 1. Monticellite microprobe
analysis, Cascade Slide, NY.

Oxide	Weight Percent	Formula	
SiO₂	36.96	O	3.990
TiO₂	0.02	Si	0.991
Al₂O₃	0.00	Al	0.000
FeO	3.89	Fe²⁺	0.087
MnO	0.39	Ti	0.000
MgO	22.79	Mg	0.911
CaO	34.86	Mn	0.009
Na₂O	0.01	Ca	1.001
Total	100.39	Na	0.000

Table 2. X-ray data for natural monticellite
$(Ca_{1.00}Mg_{0.91}Fe_{0.09}Mn_{0.01}Si_{0.99}O_{3.99})$ and
Yoder's (1968) synthetic monticellites.

natural monticellite			#4 (1350°C, 8.5 kbar)			
hkl	d(obs)	d(calc)	I	hkl	d(obs)	d(calc)	I
021	4.193	4.191	40	021	4.143	4.140	30
101	3.851	3.851	15	101	3.830	3.829	15
111	3.642	3.639	70	111	3.614	3.615	90
002	3.193	3.193	35	002	3.157	3.157	70
130	2.938	2.938	90	130	2.911	2.912	80
022	2.769	2.768	20	022	2.741	2.742	20
131	2.669	2.669	100	131	2.645	2.644	100
112	2.589	2.590	70	112	2.567	2.567	90
041	2.547	2.547	30	--	--	--	--
210	2.358	2.357	10	--	--	--	--
061	1.778	1.778	20	--	--	--	--
241	1.752	1.752	20	--	--	--	--
133	1.723	1.724	15	--	--	--	--
043	1.689	1.689	20	--	--	--	--

#160 (920°C, 2.0 kbar)			#150 (975°C, 5.0 kbar)			
021	4.177	4.178	45	021	4.177	4.176	35
101	3.844	3.844	15	101	3.843	3.842	10
111	3.629	3.632	75	111	3.631	3.630	60
130	2.933	2.931	85	130	2.929	2.930	40
022	2.761	2.730	20	--	--	--	--
131	2.662	2.663	100	131	2.662	2.661	100
112	2.582	2.584	30	112	2.580	2.582	45
041	2.538	2.539	25	--	--	--	--
122	2.398	2.395	20	122	2.395	2.394	35

#126 (1060°C, 10 kbar)						
021	4.174	4.173	15				
101	3.844	3.846	7				
111	3.633	3.633	30				
130	2.929	2.930	25				
022	2.755	2.757	7				
131	2.661	2.661	100				
112	2.582	2.583	25				
122	2.397	2.394	20				

normalized to two octahedral cations. The following equation was solved to obtain the molar volume of pure monticellite:

$$Ca_{0.997}Mg_{0.907}Fe_{0.087}Mn_{0.009}SiO_4 = 0.907CaMgSiO_4$$

natural monticellite   monticellite

$$+ 0.087CaFeSiO_4 + 0.0045Mn_2SiO_4 + 0.0015Ca_2SiO_4.$$

kirschsteinite   tephroite   Ca-olivine

(6)
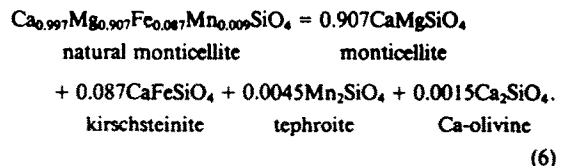
Studies of olivine solid solutions show a nearly linear variation in molar volume between end-member phases (FRANCIS and RIBBE, 1980; LUMPKIN and RIBBE, 1983; LUMPKIN *et al.*, 1983; MUKHOPADHYAY and LINDSLEY, 1983; FRANCIS, 1985). Because of the near-linearity of volumes of different olivine solid-solutions, the results are indifferent to the particular choice of "molecules" in Eqn. 6. The calculated molar volume of 51.48 ± 0.02 cm³ is in good agreement with other estimates when similarly extrapolated to ideal CaMgSiO₄ (Table 3). The calculated lattice parameters of the Cascade Slide monticellite are consistent with an ordered phase when compared with the lattice parameters of BROWN (1982) and LUMPKIN *et al.* (1983).

HEAT CAPACITY AND ENTROPY OF MONTICELLITE

The heat capacity of monticellite was measured between 9 and 350 K in the laboratory of E. F. Westrum, Jr. at the University of Michigan with a low-temperature, intermittent-heating, adiabatic calorimeter. Details of the procedure can be found in WESTRUM *et al.* (1968) and WESTRUM (1984). The data (Table 5) plot as a smooth sigmate curve with some scatter between 9 and 11 K. The data were extrapolated below 12 K from a C_p/T vs. T^2 plot. Any magnetic transitions below 12 K due to Fe and Mn substituting for Mg were not considered. The smoothed and integrated data correspond to an entropy at 298.15 K of 109.44 ± 0.16 J·mol⁻¹ K⁻¹ (Table 6).

Table 3. Lattice parameters of natural and synthetic monticellite.

X_{Ca}	X_{Mg}	X_{Fe}*	a(Å)	b(Å)	c(Å)	V(Å)^3	V^O_{298}(cm^3)	$V^{O **}_{298}$	syn/nat	ref
1.00	0.91	0.09	4.828(1)	11.108(2)	6.386(1)	342.50(8)	51.56(1)	51.48	nat	(1)
0.99	1.01	0.00	4.8209(5)	11.0911(9)	6.3726(6)	340.74(4)	51.299(6)	51.38	syn.	(2)
1.00	0.93	0.07	4.825(1)	11.111(1)	6.382(2)	342.14(10)	51.51(2)	51.43	nat.	(3)
0.965	1.035	0.00	4.820(1)	11.075(4)	6.363(1)	339.69(10)	51.15(2)	51.42	syn.	(4)
1.00	1.00	0.00	4.822	11.108	6.382	341.84	51.46	51.46	nat.	(5)
0.95	1.05	0.00	4.823(5)	11.074(7)	6.367(4)	340.07(28)	51.20(4)	51.60	syn.	(6)
0.94	1.06	0.00	4.820(5)	11.070(8)	6.363(4)	339.55(21)	51.12(4)	51.60	syn.	(7)
0.945	1.055	0.00	4.829(5)	11.057(10)	6.362(4)	339.69(27)	51.14(4)	51.58	syn.	(8)
0.85	1.15	0.00	4.815(1)	10.968(2)	6.314(2)	333.51(10)	50.11(2)	51.25	syn.	(9)

(1) This study; (2) Warner and Luth, 1973; (3) Lager and Meagher, 1978;
(4) Brousse et al., 1984; (5) Onken, 1964.
(6-9) Analyses of Yoder's (1968) run products--(6) run 160 920°C, 2 kbar;
(7) run 150 975°C, 5 kbar; (8) run 126 1060°C, 10 kbar; (9) run 4 1350°C, 8 kbar.
$X_{Ca} + X_{Mg} + X_{Fe} = 2$. * Extrapolated to end-member monticellite (see text).

The entropy of end-member monticellite was calculated with a procedure analogous to that for molar volume. Entropy data for kirschsteinite are not available, so the entropy of fayalite and calcium-olivine were substituted for kirschsteinite. A linear variation in entropy with composition between natural and end-member monticellite and the phases calcium olivine, tephroite, and fayalite was assumed (Table 4). The magnetic transition contribution to the entropies of fayalite and tephroite were subtracted from the S^0_{298} of these phases as the equivalent magnetic entropy contribution to monticellite was smoothed out of the data. The extrapolated S^0_{298} (108.1 ± 0.2 J·mol^{-1} K^{-1}) compares favorably with the estimate of VALLEY and ESSENE (1980, 107.3 J·mol^{-1} K^{-1}), but less favorably with previous estimates (HELGESON et al., 1978, 110.5 J·mol^{-1} K^{-1}; ROBIE et al., 1978, 102.5 J·mol^{-1} K^{-1}).

Heat capacity measurements from 340 to 1000 K were made with a differential scanning calorimeter at the U.S. Geological Survey in Reston, Virginia. These data were fit to the low-temperature data in the range 290–350 K and are given in Table 7. The data were smoothed (Table 8, Fig. 1) following the procedure of HEMINGWAY et al. (1981). The following heat capacity equation was fit to the data:

$$Cp(J·mol^{-1} K^{-1}) = 231.404 - 8.53144·10^{-4} T$$
$$- 1623.422T^{-0.5} - 1.24743·10^6 T^{-2} - 1.333·10^{-6} T^2.$$
$$(7)$$

An equation for the entropy of end-member monticellite as a function of temperature was calculated by the same procedure for the S^0_{298} determination, using compatible entropy coefficients for the phases calcium olivine, tephroite and fayalite (Table 4). Entropy data were extended to 1700 K using the empirical prediction method of ROBINSON and HAAS (1983) constrained by the measured entropy data below 1000 K. High temperature entropy estimates using mineral summation techniques are within 1.5 J·mol^{-1} K^{-1} using the following equations:

$$CaMgSiO_4 = 2CaSiO_3 + Mg_2SiO_4 - CaMgSi_2O_6$$
monticellite   wollastonite   forsterite   diopside

$$S^0_{1400 K} = 356.9 \text{ J·mol}^{-1} K^{-1}; \quad (8)$$

$$CaMgSiO_4 = Mg_2SiO_4 + CaO - MgO$$
monticellite   forsterite   lime   periclase

$$S^0_{1400 K} = 356.9, \quad S^0_{1500 K} = 370.0 \text{ J·mol}^{-1} K^{-1}. \quad (9)$$

The entropies of monticellite at 1400 and 1500 K using the technique of ROBINSON and HAAS (1983) are 355.8 and 368.5 J·mol^{-1} K^{-1} respectively. The following entropy equation is valid in the range 298–1700 K:

$$S^0_T(J·mol^{-1} K^{-1}) - S^0_{298} = 164.79 \ln T$$
$$+ 15.337·10^{-3} T + 22.791·10^5 T^{-2} - 968.94. \quad (10)$$

The entropy of 295.1 J·mol^{-1} K^{-1} at 1000 K using the above equation is higher than the estimate of 291–293 J·mol^{-1} K^{-1} using enthalpy data combined with experimental reversals (BROUSSE et al., 1984).

PHASE EQUILIBRIA IN THE SYSTEM CaO-MgO-SiO$_2$-CO$_2$

With new data on the entropy of monticellite, we attempted to fit the calculated curves for reactions (1–5) and the decarbonation reactions
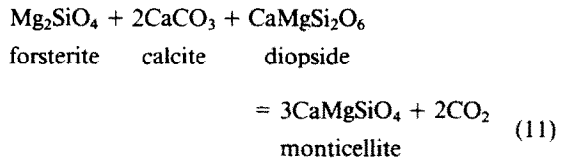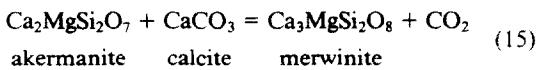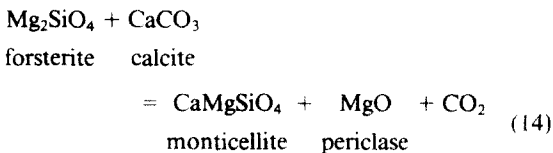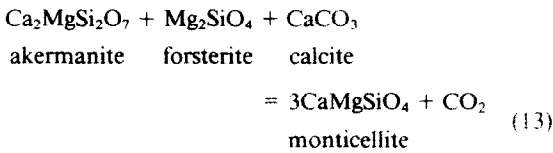
$$Mg_2SiO_4 + 2CaCO_3 + CaMgSi_2O_6$$
forsterite   calcite   diopside

$$= 3CaMgSiO_4 + 2CO_2$$
monticellite
$$(11)$$

Table 4. Volume and entropy data for olivine structures.

	V^O_{298}	Source	S^0_{298}	A	B	C	D	Source
Calcium Olivine	59.11	(2)	120.50	138.32	47.6182	13.146	-817.022	(2)
Fayalite	46.15	(2)	151.00	164.43	26.108	18.522	-965.470	(4)
Forsterite	43.65	(2)	94.11	146.99	31.291	17.344	-866.35	(5)
Kirschsteinite	52.51	(6)	136.02	133.37	56.318	7.864	-785.628	(7)
Monticellite***	51.56	(1)	109.44	152.39	29.225	17.443	-896.556	(1)
Monticellite	51.48	(1)	108.10	164.79	15.337	22.791	-968.940	(1)
Tephroite	48.61	(3)	155.90	161.71	19.610	18.966	-948.512	(5)

(1) This study; (2) Robinson et al., 1982; (3) Robie et al., 1978;
(4) Robie et al., 1982a; (5) Robie et al., 1982b;
(6) Mukhopadhyay and Lindsley, 1983; (7) 1/2 -Ca-olivine + 1/2 fayalite.
* Entropy estimate without magnetic transition contribution. ** For non-end-member monticellite (see text). *** For end-member monticellite.
(V^O_{298} in cm^3/mol; $S^0_T - S^0_{298}$ = A lnT + B·10^{-3} T + C·10^5 T^{-2} + D (T in K, S in J/(mol·K)).

Table 5. Experimental low temperature molar heat capacity measurements on natural monticellite $(Ca_{1.00}Mg_{0.91}Fe_{0.09}Mn_{0.01}Si_{0.99}O_{3.99})$.

Temp. Kelvin	Heat Capacity J/mol·K	Temp. Kelvin	Heat Capacity J/mol·K	Temp. Kelvin	Heat Capacity J/mol·K
Series I				Series IV	
		31.36	2.874		
301.67	126.9	32.81	3.276	134.64	62.34
306.69	126.2	34.32	3.711	139.63	65.17
311.86	127.0	35.91	4.234	144.68	67.93
317.01	128.0	37.58	4.814	149.74	70.64
322.20	129.3	39.33	5.444	154.82	73.21
327.40	130.5	41.04	6.110	159.90	75.69
332.61	131.0	42.84	6.845	164.99	78.45
337.81	132.7	44.86	7.725	170.08	80.69
342.97	133.4	46.97	8.696	175.02	82.95
		49.21	9.047	179.97	85.14
Series II		51.46	10.70	185.08	87.37
		53.90	12.07	190.19	89.54
(8.00)	(0.053)	56.46	13.50	195.31	91.65
(9.00)	(0.076)	59.15	15.00	200.45	92.55
(10.00)	(0.104)	61.99	16.70	205.57	95.61
(11.00)	(0.138)	64.96	18.51	210.70	97.46
(11.50)	(0.174)	67.85	20.33	215.83	99.28
(12.00)	(0.180)	70.91	22.19	220.83	101.1
12.97	0.231			225.82	102.8
13.56	0.264	Series III		230.98	104.5
12.78	0.214			236.12	106.2
13.36	0.249	68.67	20.81	241.24	107.8
13.97	0.311	71.72	23.05	246.39	109.6
14.62	0.322	75.21	24.94	244.40	108.8
15.29	0.373	78.86	27.40	249.43	110.3
15.99	0.421	82.70	30.06	254.58	111.8
16.72	0.474	86.74	32.84	259.72	113.5
17.49	0.539	90.98	35.61	264.88	114.9
18.29	0.611	95.46	38.42	270.04	116.2
19.13	0.694	100.16	41.40	275.20	117.7
20.01	0.790	105.05	44.46	280.38	119.1
20.93	0.899	114.23	50.20	285.57	120.4
21.89	1.025	119.13	53.16	290.73	121.8
22.89	1.168	124.13	56.24	295.86	123.1
23.94	1.138	129.15	59.30	301.02	124.4
25.04	1.518	134.18	62.19	306.18	125.5
26.19	1.728	139.23	64.75	311.34	126.7
27.40	1.966	144.28	67.72	316.51	127.8
28.66	2.231				
29.98	2.537				

Table 6. Molar thermodynamic properties of natural monticellite $(Ca_{1.00}Mg_{0.91}Fe_{0.09}Mn_{0.01}Si_{0.99}O_{3.99})$.

Temp. T Kelvin	Heat Capacity $C°_p$ J/mol·K	Entropy $S°_T - S°_0$ J/mol·K	Enthalpy[1] J/mol·K	Gibbs Energy Function[2] J/mol·K
15	0.349	0.133	0.088	0.042
20	0.790	0.283	0.203	0.083
25	1.505	0.532	0.387	0.141
30	2.544	0.890	0.656	0.241
40	5.712	2.020	1.490	0.532
50	10.07	3.750	2.755	0.989
60	15.51	6.053	4.417	1.833
70	21.69	8.896	6.439	2.754
80	28.21	12.22	8.750	3.680
90	34.79	15.92	11.28	5.201
100	41.27	19.92	13.95	6.680
110	47.60	24.15	16.73	8.318
120	53.74	28.56	19.56	10.08
130	59.68	33.10	22.42	11.96
140	65.36	37.73	25.28	13.94
150	70.76	42.43	28.14	15.99
160	75.85	47.16	30.96	18.12
170	80.66	51.90	33.74	20.32
180	85.19	56.65	36.48	22.56
190	89.45	61.36	39.15	24.85
200	93.46	66.06	41.77	27.18
210	97.24	70.71	44.32	29.52
220	100.8	75.31	46.81	31.89
230	104.2	79.81	49.23	34.28
240	107.4	84.37	51.59	36.68
250	110.5	88.82	53.88	39.09
260	113.5	93.21	56.12	41.50
270	116.3	97.54	58.30	43.92
280	119.0	101.8	60.41	46.34
290	121.6	106.1	62.48	48.75
298.15	123.6	109.4	64.12	50.72
300	124.1	110.2	64.49	51.16
310	126.5	114.3	66.45	53.56
320	128.8	118.4	68.36	55.95
330	131.1	122.4	70.23	58.34
340	133.0	126.3	72.05	60.72
350	134.9	130.2	73.81	63.09

[1] $(H°_T - H°_0)/T$ [2] $-(G°_T - H°_0)/T$

$$CaMgSi_2O_6 + CaCO_3 = Ca_2MgSi_2O_7 + CO_2 \qquad (12)$$
diopside   calcite   akermanite

$$Ca_2MgSi_2O_7 + Mg_2SiO_4 + CaCO_3$$
akermanite   forsterite   calcite
$$= 3CaMgSiO_4 + CO_2 \qquad (13)$$
monticellite

$$Mg_2SiO_4 + CaCO_3$$
forsterite   calcite
$$= CaMgSiO_4 + MgO + CO_2 \qquad (14)$$
monticellite   periclase

$$Ca_2MgSi_2O_7 + CaCO_3 = Ca_3MgSi_2O_8 + CO_2 \qquad (15)$$
akermanite   calcite   merwinite

to the experimental data. Reactions (2, 5, 11, 13, 14) include the phases forsterite and monticellite which display significant mutual solid solution. The location of the end-member curves determined from the experimental reversals corrected for solid solution can be estimated with the mixing parameters of ADAMS and BISHOP (1985). Their reversed experiments on the join Mg_2SiO_4-$CaMgSiO_4$ show that the miscibility gap

Table 7. Experimental high temperature heat capacity measurements on natural monticellite $(Ca_{1.00}Mg_{0.91}Fe_{0.09}Mn_{0.01}Si_{0.99}O_{3.99})$.

Temp. K	Heat Capacity J/g·K	Temp. K	Heat Capacity J/g·K	Temp. K	Heat Capacity J/g·K
Series 1		Series 3		Series 5	
420.0	0.9012	519.8	0.9719	798.?	1.081
440.0	0.9192	539.7	0.9856		
459.9	0.9343	559.7	0.9951	Series 6	
479.9	0.9489	579.6	1.006		
499.8	0.9629	599.6	1.016	848.?	1.077
519.8	0.9697	619.5	1.021		
539.7	0.9807	639.5	1.026	Series 7	
548.7	0.9866	648.5	1.030		
				897.?	1.092
Series 2		Series 4			
				Series 8	
519.8	0.9725	659.4	1.030		
539.7	0.9854	679.4	1.036	947.?	1.105
559.7	0.9921	699.3	1.038		
579.6	1.002	719.3	1.043	Series 9	
599.6	1.011	739.3	1.055		
619.5	1.015	748.2	1.059	997.?	1.114
639.5	1.026				
648.5	1.027			Series 10	
				340.?	0.8305
				350.?	0.8445
				360.?	0.8587

Table 8. Thermodynamic properties of ideal monticellite ($CaMgSiO_4$). Formula weight 156.469

Temp. T Kelvin	Heat Capacity C_p° J/mol·K	Entropy $S_T^\circ - S_0^\circ$ J/mol·K	Enthalpy[1] Function J/mol·K	Gibbs[2] Energy Function J/mol·K	Gibbs[3] Free Energy kJ/mol
298.15	123.0	108.1	0.000	108.1	-2133.1
uncertainty	±0.2			±0.2	
300	123.4	108.9	0.760	108.1	-2132.4
350	134.0	128.7	19.078	109.6	-2112.6
400	141.9	147.2	33.957	113.2	-2092.8
450	148.1	164.2	46.305	117.9	-2073.1
500	153.1	180.1	56.738	123.4	-2053.3
550	157.2	194.9	65.687	129.2	-2033.6
600	160.7	208.7	73.461	135.3	-2013.9
650	163.7	221.7	80.288	141.4	-1994.2
700	166.2	233.9	86.337	147.6	-1974.6
750	168.5	245.5	91.742	153.7	-1954.9
800	170.5	256.4	96.604	159.8	-1935.3
850	172.3	266.8	101.01	165.8	-1915.7
900	173.9	276.7	105.01	171.7	-1896.2
950	175.3	286.1	108.68	177.5	-1878.4
1000	176.6	295.2	112.04	183.1	-1862.3

[1] $(H_T^\circ - H_{298}^\circ)/T$ [2] $-(G_T^\circ - H_{298}^\circ)/T$ [3] G_T° (elements)

Transitions in reference state elements
    Calcium...alpha-beta-720 K,
    Magnesium...melting point-922 K.

between forsterite and monticellite is independent of pressure and is asymmetric, with the monticellite limb displaying greater solid solution. Activities of monticellite and forsterite at various temperatures were calculated from the one-site asymmetric solution model of ADAMS and BISHOP (1985). At the temperatures of Yoder's experiments (Fig. 2) for reactions (2) and (5),

the amount of solid solution predicted by ADAMS and BISHOP's model (e.g. a_{Mo} = 0.92, a_{Fo} = 0.96 at 1500 K) shifts the experimental reversals significantly relative to end-member monticellite and forsterite.

The degree of solid solution for the phases akermanite and diopside in the $CaO-MgO-SiO_2$ system should be minimal (KUSHIRO and SCHAIRER, 1964; SCHAIRER et al., 1967; VALLEY and ESSENE, 1980). Since the knowledge of the solid solutions is critical for proper location of the end-member reaction curves, Dr. Yoder has kindly provided the run-products of reactions (2) and (5) for analysis. The X-ray analysis of monticellite synthesized with forsterite at 1350°C and 8 kbar (Table 2) corresponds to a completely ordered olivine of composition $Mo_{85}Fo_{15}$ using the a-b plot for Ca-Mg olivines of LUMPKIN et al. (1983). Compositions of the same sample determined by electron microprobe analyses range from Mo_{82-85} (Table 9). The composition expected from the model of ADAMS and BISHOP (1985) is $Mo_{86}Fo_{14}$, in agreement with the compositions of Yoder's run products. Microprobe analyses of monticellites synthesized at lower temperatures give a much wider range of compositions. A monticellite synthesized at 975°C and 5 kbar by YODER (1968), has an apparent compositional range of Mo_{75-96} (Table 9). Back-scattered electron imaging of this monticellite shows it to contain many blebs of forsterite and some akermanite. The most monticellite-rich analysis of this sample ($Mo_{96}Fo_4$) corresponds precisely with the composition predicted by the Margules parameters and X-ray determinative methods of
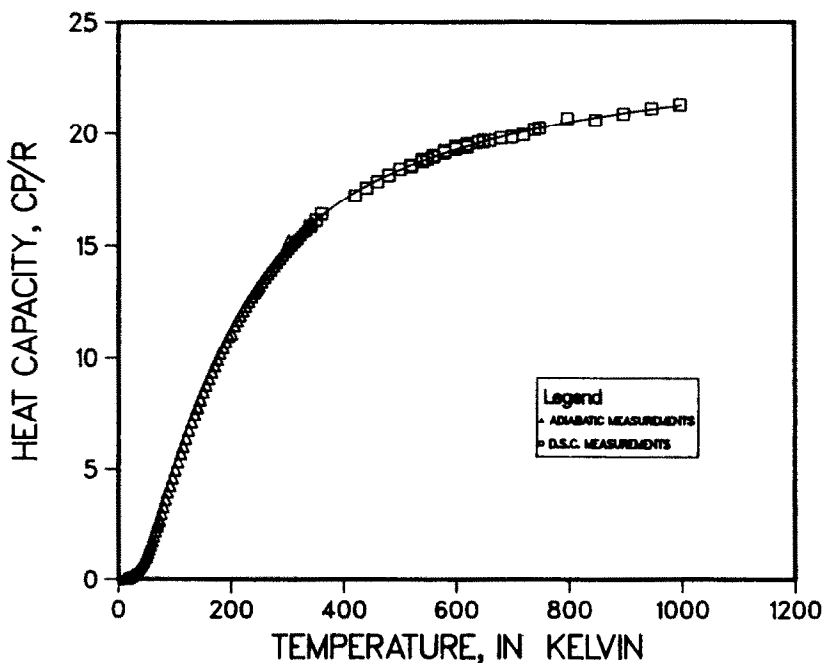
HEAT CAPACITY OF MONTICELLITE

FIG. 1. Low- and high-temperature heat capacity data for natural monticellite ($Ca_{1.00}Mg_{0.91}Fe_{0.09}Mn_{0.01}Si_{0.99}O_{3.99}$). The solid line from 298 to 1000 K shows the smoothing function fit to the experimental data.
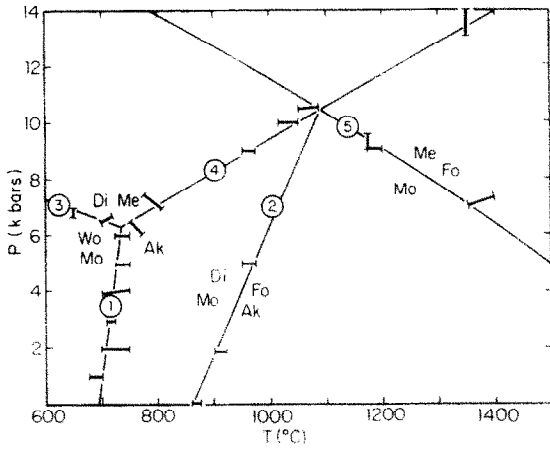
FIG. 2. Pressure-temperature diagram for reactions (1) through (5) for end-member phases. Reversed brackets for reactions (2) and (5) are corrected for solid solution. The univariant points $-Fo$ and $-Wo$ are located at 735°C (1008 K) and 6.3 kbar and 1088°C (1361 K) and 10.2 kbar respectively. Reversals are from the following sources: $Wo + Mo = Ak$ (HARKER and TUTTLE, 1956; YODER, 1968); $Mo + Di = Fo + Ak$ (WALTER, 1963a; YODER, 1968); $Mo = Me + Fo$ (YODER, 1968); $Di + Me = Ak$ (KUSHIRO and YODER, 1964; YODER, 1968); $Di + Me = Wo + Mo$ (YODER, 1968). Abbreviations used (as in all tables) are: Ak = akermanite, Cc = calcite, Di = diopside, Fo = forsterite, Me = merwinite, Mo = monticellite, Pe = periclase, Wo = wollastonite. The reversal directly above the univariant point $-Wo$ is for the reaction $Di + Mo = Fo + Ak$.

ADAMS and BISHOP (1985). Analyses with greater apparent solid solution are likely due to contamination by the small forsterite inclusions. Alternatively, the variation observed in the microprobe analyses may be caused by metastable reaction products in experiments run at lower temperature and pressure.

YODER (1973, 1975) suggested that akermanite may exhibit solid solution with other phases in the CaO-

MgO-SiO₂ system. Analyses of akermanite from run products show a consistent enrichment in Mg relative to Ca (Table 9), but a constant (Ca + Mg)/Si ratio of 3/2 indicating no detectable solid solution toward olivine. Merwinite analyses show solid solution toward forsterite with an Mg/(Ca + Mg) ratio of 0.26 (vs. 0.25 for ideal merwinite), but the (Ca + Mg)/Si ratio of 2 suggests that merwinite has no solid solution off the Ca₂SiO₄-Mg₂SiO₄ join. Diopside coexisting with forsterite and monticellite may show some solid solution toward enstatite at high temperatures. The diopside analysis (Table 9) is deficient in silica, but monticellite analyzed in the same sample also shows a deficiency in silica, indicating possible analytical errors for silicon. Experiments on the akermanite-diopside join show very slight solid solution of diopside toward akermanite at 1300°C (KUSHIRO and SCHAIRER, 1964), supported by VALLEY and ESSENE's (1980) analysis of diopside coexisting with akermanite from the experimental run products of YODER (1968). This solid solution requires a vacancy related substitution that is not well understood. For the purposes of this paper only the following solid solution effects involving Mg-Ca substitutions will be considered:

1) Monticellite and forsterite exhibit mutual solid solution as defined by ADAMS and BISHOP (1985);

2) Akermanite shows ~2% Mg/Ca enrichment, but maintains a stoichiometric (Ca + Mg)/Si ratio of 3/2;

3) Merwinite shows 3–4% solid solution toward forsterite, but maintains a (Ca + Mg)/Si ratio of 2;

4) Diopside shows slight solid solution toward enstatite [Mg/(Ca + Mg)] and may also lie off the diopside-enstatite join toward akermanite.

For reaction (2) the shift due to solid solution can be evaluated from the equation

$$\Delta G_T^{P_2} - \Delta G_T^{P_1} = \int_{P_1}^{P_2} \Delta V dP + RT \ln \frac{(a_{ak})^3(a_{fo})^3}{(a_{di})(a_{mo})^3} . \quad (16)$$

Table 9. Electron microprobe analyses of Yoder's (1968) experimental run products.

phase/run #	mo 4	fo 4	mo 150	ak 150	mo 167	fo 167	ak ?	me ?
T°C-P kb	1350/8.0	1350/8.0	975/5.0	1075/10.5	1075/10.5	1075/10.5	1400/9.0	1400/9.0
coex. phases	ak,fo	ak,fo	ak,fo	ak,fo	ak,fo	ak,fo	fo,me	fo,ak
SiO₂	38.36	41.82	39.01	43.96	39.49	42.50	44.21	36.75
MgO	31.54	53.11	27.71	14.98	27.15	56.06	15.28	13.60
CaO	31.12	4.05	35.39	41.15	33.54	2.38	40.99	50.05
total	101.02	98.98	102.11	100.10	100.18	100.94	100.48	100.4
Si	0.969	1.001	0.990	1.991	1.022	0.991	1.993	1.993
Mg	1.188	1.895	1.048	1.012	1.048	1.949	1.023	1.100
Ca	0.843	0.104	0.962	1.997	0.930	0.059	1.980	2.908
O	3.969	4.001	3.990	6.991	4.022	3.991	6.993	7.994

phase/run #	mo 163	fo 163	me 162	mo 162	fo 162	ak 162	di 126	mo 125
T°C-P kb	1175/10.0	1175/10.0	1175/10.0	1175/10.5	1175/10.5	1175/10.5	1060/10.0	1060/10.0
coex. phases	fo,ak	mo,ak	mo,fo,ak	fo,ak,me	mo,ak,me	mo,fo,me	mo,fo	di,fo
SiO₂	39.17	42.23	36.84	38.19	42.34	44.15	53.50	37.62
MgO	31.79	55.16	13.40	30.92	55.72	15.15	19.61	26.71
CaO	28.53	4.00	49.39	29.11	3.89	40.70	26.01	33.84
total	99.49	101.39	99.64	98.22	101.95	100.00	99.12	100.21
Si	1.004	0.984	2.014	0.992	0.980	2.000	1.935	0.967
Mg	1.214	1.916	1.092	1.197	1.923	1.023	1.057	1.102
Ca	0.783	0.100	2.893	0.810	0.096	1.976	1.008	0.932
O	4.003	3.984	8.014	3.992	3.980	7.000	5.935	3.967

The shift in the other reactions due to solid solution can be estimated with similar equations. Akermanite, merwinite and diopside activities are taken as atom fraction over all octahedral sites. For reactions (2) and (4), the effects of solid solution for akermanite, merwinite and diopside tend to cancel each other and the net shift for both reactions is less than 0.1 kbar. For reaction (5), the solid solution between monticellite, forsterite and merwinite places the theoretical end-member reversal brackets at significantly higher pressures (2 kbar at 1400°C).

The effect of solid solution for the location of the decarbonation reaction reversals is very small at the temperature of the experiments. With the constraints of the reversal brackets corrected for solid solution, the P-T location of reactions (1–5) for the ideal phases was calculated with the aid of the computer program EQUILI (WALL and ESSENE, unpublished) from the relation

$$\Delta G_{T2}^{P2} - \Delta G_{T1}^{P1} = \int_{P_1}^{P_2} \Delta V dP - \int_{T_1}^{T_2} \Delta S dT. \quad (17)$$

Data for all phases are given in Table 10. The two solid-solid reaction invariant points, forsterite-absent (−Fo) and wollastonite-absent (−Wo) in Fig. 2 are located at 1008 ± 5 K and 6.3 ± 0.1 kbar and 1361 ± 10 K and 10.2 ± 0.2 kbar respectively. The entropies of all phases considered are now well-known except for merwinite, which has only been measured down to 52 K (WELLER and KELLEY, 1963). The entropy estimate of WELLER and KELLEY for merwinite results in a poor fit of the generated curves to the experimental reversals

corrected for solid solution. A best fit is made when the S_{298}^0 of merwinite is set at 250.2 J · mol^{-1} K^{-1}, less than WELLER and KELLEY's estimate of 253.2 J · mol^{-1} K^{-1}. WELLER and KELLEY (1963) noted a small transition at 122 K which may be due to a phase transition or contamination by other phases. The X-ray pattern of their synthetic merwinite had two peaks that do not correspond to merwinite. The discrepancy between the measured and calculated entropy of merwinite may be due to possible contamination by other phases and to errors in the extrapolation of WELLER and KELLEY's (1963) heat capacity from 50 to 0 K.

The best fit of reactions (1–5, 11–15) to the experimental reversals and the ΔG_{298}^0 of each phase was determined in the following way:

1) The ΔG_{298}^0 was calculated for each reaction (1–5, 11–15) from the reversals at high P-T. For the decarbonation reactions, using the modified Redlich-Kwong model of KERRICK and JACOBS (1981) for H_2O-CO_2 mixing, the experiments with pure CO_2 and at low pressures are inconsistent with the experiments with H_2O-CO_2 mixtures at 1 kbar.

2) Simultaneous calculation does not yield a unique solution for the ΔG_{298}^0 of each phase. The ΔG_{298}^0 of CO_2, calcite, periclase and wollastonite were assumed to be correct (ROBINSON et al., 1982; TREIMAN and ESSENE, 1983), and with these data the ΔG_{298}^0 of the remaining phases were calculated.

The best fit for reactions (1–5, 11–15) is shown in Figs. 2–4 using the thermodynamic data in Table 10. The free energy of monticellite (ΔG_{298}^0) is calculated as −2133 kJ · mol^{-1}, significantly less than previously re-

Table 10. Thermodynamic data of minerals used in EQUILI.

Volume and entropy: (V_{298}^0 in cm^3/mol; $S_T^0 - S_{298}^0 = A \cdot \ln T + B \cdot 10^{-3} T + C \cdot 10^5 \cdot T^{-2} + D$
(T in K, S in J/(mol·K), ΔG in kJ/mol)

	V_{298}^0	ref.	S_{298}^0	A	B	C	D	ref.	ΔG_{298}^0	ref.
Akermanite	92.51	(1)	212.5	242.59	55.184	20.521	-1421.43	(1)	-3667	(7)
Calcite	36.92	(18)	91.78	102.91	23.435	12.211	-607.06	(5)	-1131	(20)
Diopside	66.11	(3)	142.7	230.95	22.792	34.463	-1361.34	(4)	-3025	(7)
Forsterite	43.65	(5)	94.1	151.49	26.558	19.432	-892.80	(16)	-2051	(7)
Merwinite	98.47	(6)	250.2	307.06	48.459	31.084	-1798.99	(2)	-4317	(7)
Monticellite	51.48	(7)	108.1	164.79	15.337	22.791	-968.94	(7)	-2133	(7)
Periclase	11.24	(5)	26.95	48.28	4.021	5.817	-282.79	(5)	- 569	(5)
Wollastonite	39.89	(4)	81.69	102.24	28.446	13.444	-605.87	(4)	-1549	(5)

Expansivity and Compressibility: ($V_T^0 = V_{298}^0 + V_{298}^0$ (a + b·(T-273) + c·(T-273)^2 +

d·(T-273)^3)/100; $V_{298}^P = V_{298}^0$·(1 - m·10^{-3}·P + n·10^{-6}·P^2)   (T in K, P in kbar)

	a·10^{-2}	b·10^{-3}	c·10^{-7}	d·10^{-10}	ref.	m	n	ref.
Akermanite	-0.639	1.921	18.936	-7.118	(1)	0.535	8.116	(9)
Calcite	-2.174	0.547	31.074	-6.687	(18)	1.367	3.9	(11)
Diopside	9.535	4.005	-14.196	7.626	(10)	1.108	11.02	(3,11,12)
Forsterite	8.770	2.948	14.369	-4.378	(15)	0.877	4.060	(5,15)
Merwinite	5.387	2.245	25.628	-9.927	(8)	1.108	11.02	(19)
Monticellite	6.951	2.759	8.651	-2.066	(13)	0.759	6.705	(14)
Periclase	-7.606	3.888	-3.100	-1.309	(5)	0.598	1.00	(11)
Wollastonite	11.18	5.008	-41.664	15.535	(5)	1.465	9.819	(17)

(1) Hemingway et al., 1985 (valid above 357.9 K); (2) Robie et al., 1978;
(3) Levien and Prewitt, 1981; (4) Krupka et al., 1985 a,b; (5) Robinson et al., 1982;
(6) Moore and Araki, 1972; (7) This study; (8) Skinner, 1966; (9) Gehlenite data from
Robinson et al., 1982; (10) Cameron et al., 1973; (11) Birch, 1966;
(12) Hazen and Finger, 1981; (13) Lager and Meagher, 1978;
(14) 1/2 forsterite + 1/2 calcium-olivine; (15) Hazen, 1976;
(16) Robie et al., 1982b; (17) Vaidya et al., 1973; (18) Markgraf and Reeder, 1985;
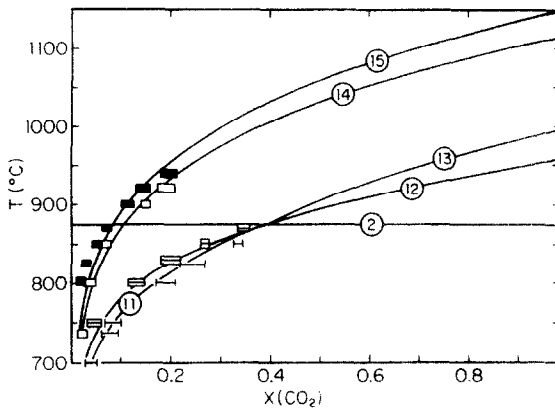(19) Used value for diopside; (20) Treiman and Essene, 1983.

FIG. 3. Temperature-$X(CO_2)$ diagram at 1 kbar total pressure. Reversals are from ZHARIKOV *et al.* 1977. Reaction numbers are as follows: (2) $Di + Mo = Fo + Ak$, (11) $Fo + Di + Cc = Mo + CO_2$, (12) $Di + Cc = Ak + CO_2$, (13) $Ak + Fo + Cc = Mo + CO_2$, (14) $Fo + Cc = Mo + Pe + CO_2$, (15) $Ak + Cc = Me + CO_2$. See Fig. 2 for abbreviations.

ported (HELGESON *et al.*, 1978, -2143 kJ $\cdot$ mol^{-1} and ROBIE *et al.*, 1978, -2146 kJ $\cdot$ mol^{-1}). The close agreement between their two estimates is a result of their use of the same enthalpy data for monticellite. More recent enthalpy measurements on monticellite by alkali borate solution calorimetry at 1073 K (BROUSSE *et al.*, 1984) were extrapolated to 298 K with the new entropy data. The $\Delta G^0_{298}(Mo)$ value of -2129 kJ $\cdot$ mole^{-1} is in excellent agreement with the present results.

The ΔG^0_{298} calculated for akermanite is -3667 kJ $\cdot$ mol^{-1} compared to -3681, -3679, and -3668 kJ $\cdot$ mol^{-1} of HELGESON *et al.* (1978), ROBIE *et al.* (1978), and HEMINGWAY *et al.* (1985) respectively. The $\Delta G^0_{1000\,K}(Ak) = -3218$ value is in good agreement with the $\Delta G^0_{1000\,K}(Ak) = -3210$ kJ $\cdot$ mol^{-1} K^{-1} determined from the solution calorimetry data of BROUSSE *et al.* (1984). The calculated ΔG^0_{298} for merwinite is -4317 kJ $\cdot$ mol^{-1}, 0.5% less than the estimates of -4339 kJ $\cdot$ mole^{-1} from ROBIE *et al.* (1978) and -4340 kJ $\cdot$ mol^{-1} from HELGESON *et al.* (1978), and 0.2% greater than the estimate of -4307 kJ $\cdot$ mol^{-1} calculated from the high-temperature enthalpy data of BROUSSE *et al.* (1984) and the entropy data in Table 10. Reaction (5) is located 2.5 kbar higher than the best fit location at 1200°C using the enthalpy data of BROUSSE *et al.* (1984). This illustrates the uncertainties in locating solid-solid reactions with enthalpy data alone. An error of just 0.2% in the enthalpy of a phase can result in a significant error in the location of a reaction curve. For these reactions, measured thermodynamic quantities must be combined with the experimental reversals to yield accurate results.

The locations of the univariant reactions (1–5, 11–15), calculated from the data in Table 10 are in excellent agreement with all of the experimental reversals (Figs. 2–4) except for reactions (14) and (15) (Fig. 4). The apparent reversals for reactions (11–14) (WALTER, 1963a,b) nearly coincide, while the calculated positions for these curves indicate that reaction (14) must lie at

higher temperatures than the other three (Fig. 4). This same conclusion was reached by TURNER (1968, p. 135) on the basis of natural occurrences and thermodynamic calculations.

Phase equilibria in the system CaO-MgO-SiO$_2$-CO$_2$ are pertinent to calc-silicates metamorphosed at high temperatures and low pressures. Monticellite, akermanite, merwinite, and monticellite + periclase are all stable in the pyroxene-hornfels facies. Their stability is controlled primarily by $P(CO_2)$ and they provide far better CO_2 barometers than thermometers.

Although there are many reports of high-temperature Ca-Mg silicates, few authors have systematically described the sequence of high-temperature assemblages around a contact aureole. JOESTEN (1974, 1976) reports assemblages of Ca- and Ca-Mg silicates in a limestone sequence intruded by a high-level gabbro. He infers temperatures of 900–1000°C based on phase equilibria involving calc-silicates (see also TREIMAN and ESSENE, 1983). JOESTEN (1976) reports a melilite (Ak_{30})-Cc-Me assemblage which is buffered by reaction (15) for a given $a(Ak)$ and $f(CO_2)$. He also reports spurrite-rankinite-wollastonite in skarns. These two assemblages may indicate skarn formation at water-rich conditions $(X(H_2O) = 0.8$–$0.95)$ and lower temperatures (850–900°C) than inferred by JOESTEN. These water-rich conditions are also expected for the formation of vesuvianite (VALLEY *et al.*, 1985) which is widespread in the skarn studied by JOESTEN. Independent thermometry is needed before more precise fluid compositions can be reliably obtained.

BOWEN (1940) estimated the relative abundance of phases in the system CaO-MgO-SiO$_2$-CO$_2$ by correlating the abundance of each mineral to its year of discovery. Diopside was named in 1806, wollastonite in 1822, forsterite in 1824, monticellite in 1831, akermanite in 1884 and merwinite in 1921, and the low-temperature calorimetry for each of these phases has to date been measured in the same order. Merwinite was the last named and it remains the only one in this
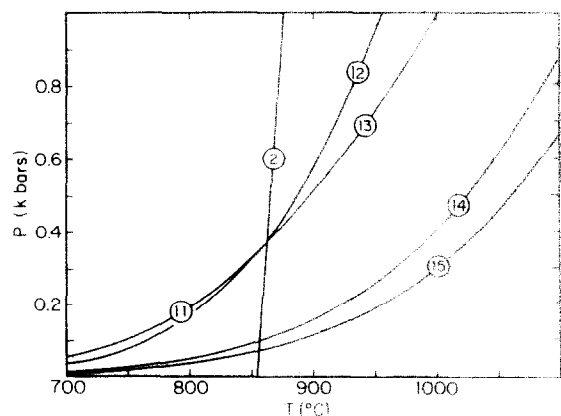

FIG. 4. Pressure-temperature diagram for decarbonation reactions. See Fig. 3 for reaction numbers. Reactions (11–13) coincide with the experimental reversals of WALTER (1963a). Reactions (14–15) are located at higher temperatures than the reversals of WALTER (1963b) and SHMULOVICH (1969).

group that does not have low-temperature calorimetry measurements.

REFERENCES

ADAMS G. E. and BISHOP F. B. (1985) An experimental investigation of thermodynamic mixing properties and unit-cell parameters of forsterite-monticellite solid solution. *Amer. Mineral.* **70,** 714–722.

BIGGAR G. M. and O'HARA M. J. (1969) Monticellite and forsterite crystalline solutions. *J. Amer. Ceram. Soc.* **52,** 249–252.

BIRCH F. (1966) Compressibility: elastic constants. In *Handbook of Physical Constants* (ed. S. P. CLARK, JR.), pp. 97–174. Geological Society America Memoir 97.

BOWEN N. L. (1940) Progressive metamorphism of siliceous limestones and dolomite. *J. Geol.* **68,** 225–274.

BROUSSE C., NEWTON R. C. and KLEPPA O. J. (1984) Enthalpy of formation of forsterite, enstatite, akermanite, monticellite and merwinite at 1073 K determined by borate solution calorimetry. *Geochim. Cosmochim. Acta* **48,** 1081–1088.

BROWN G. E., JR. (1982) Olivine and silicate spinels. In *Orthosilicates* (ed. P. H. RIBBE), pp. 275–381. Mineralogical Society of America.

CAMERON M., SUENO S., PREWITT C. T. and PAPIKE J. J. (1973) High-temperature crystal chemistry of acmite, diopside, hedenbergite, jadeite, spodumene, and ureyite. *Amer. Mineral.* **58,** 594–618.

FRANCIS C. A. (1985) New data on the forsterite-tephroite series. *Amer. Mineral.* **70,** 568–575.

FRANCIS C. A. and RIBBE P. H. (1980) The forsterite-tephroite series: I. Crystal structure refinements. *Amer. Mineral.* **65,** 1263–1269.

HARKER R. J. and TUTTLE O. F. (1956) The lower limit of stability of akermanite (Ca$_2$MgSi$_2$O$_7$). *Amer. J. Sci.* **254,** 468–478.

HAZEN R. M. (1976) Effects of temperature and pressure on the crystal structure of forsterite. *Amer. Mineral.* **61,** 1280–1293.

HAZEN R. M. and FINGER L. W. (1981) Crystal structure of diopside at high temperature and pressure. *Carnegie Inst. Wash. Yearb.* **80,** 373–376.

HELGESON H. C., DELANY J. M., NESBITT H. W. and BIRD D. K. (1978) Summary and critique of the thermodynamic properties of rock-forming minerals. *Amer. J. Sci.* **278-A,** 1–229.

HEMINGWAY B. S., KRUPKA K. A. and ROBIE R. A. (1981) Heat capacity of the alkali feldspars between 350 and 1000 K from differential scanning calorimetry, the thermodynamic functions of the alkali feldspars from 298.15 to 1400 K, and the reaction quartz + jadeite = analbite. *Amer. Mineral.* **66,** 1202–1216.

HEMINGWAY B. S., EVANS H. T., JR., NORD G. L., JR., HASELTON H. T., JR., ROBIE R. A. and McGEE J. J. (1986) A study of phase transitions in the heat capacity and thermal

expansion of akermanite, Ca$_2$MgSi$_2$O$_7$, and revised values for the thermodynamic properties of akermanite. *Can. Mineral.* (in press).

JOESTEN R. (1974) Metasomatism and magmatic assimilation at a gabbro-limestone contact, Christmas Mountains. Big Bend Region, Texas. Ph.D. dissertation, California Institute of Technology.

JOESTEN R. (1976) High-temperature contact metamorphism of carbonate rocks in a shallow crustal environment, Christmas Mountain, Big Bend region, Texas. *Amer. Mineral.* **61,** 776–781.

KERRICK D. M. and JACOBS G. K. (1981) A modified Redlich-Kwong equation for H$_2$O, CO$_2$, and H$_2$O-CO$_2$ mixtures at elevated pressures and temperatures. *Amer. J. Sci.* **281,** 735–767.

KRUPKA K. M., HEMINGWAY B. S., ROBIE R. A. and KERRICK D. M. (1985a) High-temperature heat capacities and derived thermodynamic properties of anthophyllite, diopside, dolomite, enstatite, bronzite, talc, tremolite and wollastonite. *Amer. Mineral.* **70,** 261–271.

KRUPKA K. M., ROBIE R. A., HEMINGWAY B. S., KERRICK D. M. and ITO J. (1985b) Low-temperature heat capacities and derived thermodynamic properties of anthophyllite, diopside, enstatite, bronzite, and wollastonite. *Amer. Mineral.* **70,** 249–260.

KUSHIRO I. and SCHAIRER J. F. (1964) The join diopside-akermanite. *Carnegie Inst. Wash. Yearb.* **63,** 132–133.

KUSHIRO I. and YODER H. S., JR. (1964) Breakdown of monticellite and akermanite at high pressures. *Carnegie Inst. Wash. Yearb.* **63,** 81–83.

LAGER G. A. and MEAGHER E. P. (1978) High-temperature structural study of six olivines. *Amer. Mineral.* **63,** 365–377.

LEVIEN L. and PREWITT C. T. (1981) High-pressure structural study of diopside. *Amer. Mineral.* **66,** 315–323.

LUMPKIN G. R. and RIBBE P. H. (1983) Composition, order-disorder and lattice parameters of olivines: relationships in silicate, germanate, beryllate, phosphate and borate olivines. *Amer. Mineral.* **68,** 164–176.

LUMPKIN G. R., RIBBE P. H. and LUMPKIN N. E. (1983) Composition, order-disorder and lattice parameters of olivines: determinative methods for Mg-Mn and Mg-Ca silicate olivines. *Amer. Mineral.* **68,** 1174–1182.

MARKGRAF S. A. and REEDER R. J. (1985) High-temperature structure refinements of calcite and magnesite. *Amer. Mineral.* **70,** 590–600.

MOORE P. B. and ARAKI T. (1972) Atomic arrangement of merwinite, Ca$_3$Mg(SiO$_4$)$_2$, an unusual dense-packed structure of geophysical interest. *Amer. Mineral.* **57,** 1355–1374.

MUKHOPADHYAY D. K. and LINDSLEY D. H. (1983) Phase relations in the join kirschsteinite (CaFeSiO$_4$)-fayalite (Fe$_2$SiO$_4$). *Amer. Mineral.* **68,** 1089–1094.

ONKEN H. (1964) Verfeinerung der Kristallostruktur von Monticellite. *Naturwissenschaften* **51,** 334.

ROBIE R. A., HEMINGWAY B. S. and FISHER J. R. (1978) Thermodynamic properties of minerals and related substances at 298.15 K and 1 bar (10^5 pascals) pressure and at higher temperatures. *U. S. Geol. Surv. Bull.* **1452,** 456 p. (reprinted with corrections).

ROBIE R. A., FINCH C. B. and HEMINGWAY B. S. (1982a) Heat capacity and entropy of fayalite (Fe$_2$SiO$_4$) between 5.1 and 383 K: comparison of calorimetric and equilibrium values for the QFM buffer reaction. *Amer. Mineral.* **67,** 463–469.

ROBIE R. A., HEMINGWAY B. S. and TAKEI H. (1982b) Heat capacities and entropies of Mg$_2$SiO$_4$, Mn$_2$SiO$_4$, and Co$_2$SiO$_4$ between 5 and 380 K. *Amer. Mineral.* **67,** 470–482.

ROBINSON G. R., JR. and HAAS J. L., JR. (1983) Heat capacity, relative enthalpy, and calorimetric entropy of silicate minerals: an empirical method of prediction. *Amer. Mineral.* **68,** 541–554.

ROBINSON G. R., JR., HAAS J. L., JR., SCHAFER C. M. and HASELTON H. T., JR. (1982) Thermodynamic and ther-

mophysical properties of selected phases in the MgO-SiO$_2$-H$_2$O-CO$_2$, CaO-Al$_2$O$_3$-SiO$_2$-H$_2$O-CO$_2$, and Fe-FeO-Fe$_2$O$_3$-SiO$_2$ chemical systems, with special emphasis on the properties of basalts and their mineral components. *U. S. Geol. Surv. Open-File Rept. 83-79*, 429 p.

SCHAIRER J. F., YODER H. S., JR. and TILLEY C. E. (1967) The high-temperature behaviour of synthetic melilites on the join gehlenite-soda melilite-akermanite. *Carnegie Inst. Wash. Yearb.* **65**, 217–226.

SHMULOVICH K. I. (1969) Stability of merwinite in the system CaO-MgO-SiO$_2$-CO$_2$. *Doklady. Earth Sci. Sect.* **184**, 125–127.

SKINNER B. J. (1966) Thermal expansion. In *Handbook of Physical Constants.* (ed. S. P. CLARK, JR., pp. 75–96. Geological Society America Memoir 97.

TREIMAN A. H. and ESSENE E. J. (1983) Phase equilibria in the system CaO-SiO$_2$-CO$_2$. *Amer. J. Sci.* **283-A**, 97–121.

TURNER F. J. (1968) *Metamorphic Petrology.* McGraw-Hill, Inc. 1st edn. 403 p.

VAIDYA S. N., BAILEY S., PASTERNACK T. and KENNEDY G. C. (1973) Compressibility of fifteen minerals to 45 kilobars. *J. Geophys. Res.* **78**, 6893–6898.

VALLEY J. W. and ESSENE E. J. (1980) Akermanite in the Cascade Slide Xenolith and its significance for regional metamorphism in the Adirondacks. *Contrib. Mineral. Petrol.* **74**, 143–152.

VALLEY J. W., PEACOR D. R., BOWMAN J. R., ESSENE E. J. and ALLARD M. J. (1985) Crystal chemistry in the system CaO-MgO-Al$_2$O$_3$-SiO$_2$-H$_2$O-CO$_2$. *J. Metamorphic Geol.* **3**, 137–153.

WALTER L. S. (1963a) Experimental studies on Bowen's decarbonation series: Part I: P-T univariant equilibria of the "monticellite" and "akermanite" reactions. *Amer. J. Sci.* **261**, 488–500.

WALTER L. S. (1963b) Experimental studies on Bowen's decarbonation series: Part II: P-T univariant equilibria of the

reaction: forsterite + calcite = monticellite + periclase + CO$_2$. *Amer. J. Sci.* **261**, 773–779.

WARNER R. D. and LUTH W. C. (1973) Two-phase data for the join monticellite (CaMgSiO$_4$)-forsterite (Mg$_2$SiO$_4$): experimental results and numerical analysis. *Amer. Mineral.* **58**, 998–1008.

WELLER W. W. and KELLEY K. K. (1963) Low-temperature heat capacities and entropies at 298.15°K of akermanite, cordierite, gehlenite, and merwinite. *U. S. Bur. Mines Rept. Inv. 6343*, 7 p.

WESTRUM E. F., FURUKAWA G. T. and McCULLOUGH J. P. (1968) Adiabatic low temperature calorimetry. In *Experimental Thermodynamics* (eds. J. P. McCULLOUGH AND D. W. SCOTT). Vol. 1, pp. 133–214. Butterworths and Co., Ltd.

WESTRUM E. F., JR. (1984) Computerized adiabatic thermophysical calorimetry. In *Proceedings NATO Advanced Study Institute on Thermochemistry at Viana de Castello, Portugal* (ed. M. A. V. RIBERIO DA SILVA), pp. 745–776 New York.

YANG H. Y. (1973) New data on forsterite and monticellite solid solutions. *Amer. Mineral.* **58**, 343–345.

YODER H. S., JR. (1968) Akermanite and related melilite-bearing assemblages. *Carnegie Inst. Wash. Yearb.* **66**, 471–477.

YODER H. S., JR. (1973) Melilite stability and paragenesis. *Fortschr. Mineral.* **50**, 140–173.

YODER H. S., JR. (1975) Relationship of melilite-bearing rocks to kimberlite: a preliminary report on the system akermanite-CO$_2$. *Phys. Chem. Earth* **9**, 883–894.

ZHARIKOV V. A., SHMULOVICH K. I. and BULATOV V. K. (1977) Experimental studies in the system CaO-MgO-Al$_2$O$_3$-SiO$_2$-CO$_2$-H$_2$O and conditions of high-temperature metamorphism. In *Experimental Petrology Related to Extreme Metamorphism* (ed. D. H. GREEN). *Tectonophysics* **43**, 145–162.